ACS SENSORS

Article

Cite This: ACS Sens. 2019, 4, 1346−1357

pubs.acs.org/acssensors

Label-Free Optical Detection of Multiple Biomarkers in Sweat, Plasma, Urine, and Saliva

Prajokta Ray and Andrew J. Steckl*

Nanoelectronics Laboratory, University of Cincinnati, Cincinnati, Ohio 45221-0030, United States of America

Supporting Information

ABSTRACT: We report a novel label-free quantitative detection of human performance "stress" biomarkers in different body fluids based on optical absorbance of the biomarkers in the ultraviolet (UV) region. Stress biomarker (hormones and neurotransmitters) concentrations in bodily fluids (blood, sweat, urine, saliva) predict the physical and mental state of the individual. The stress biomarkers primarily focused on in this manuscript are cortisol, serotonin, dopamine, norepinephrine, and neuropeptide Y. UV spectroscopy of stress biomarkers performed in the 190−400 nm range has revealed primary and secondary absorption peaks at near-UV wavelengths depending on their molecular structure. UV characterization of individual and multiple biomarkers is reported in various biofluids. A microfluidic/optoelectronic platform for biomarker detection is reported, with a prime focus toward cortisol evaluation. The current limit of detection of cortisol in sweat is ∼200 ng/mL (∼0.5 μM), which is in the normal (healthy) range. Plasma samples containing both serotonin and cortisol resulted in readily detectable absorption peaks at 203 (serotonin) and 247 (cortisol) nm, confirming feasibility of simultaneous detection of multiple biomarkers in biofluid samples. UV spectroscopy performed on various stress biomarkers shows a similar increasing absorption trend with concentration. The detection mechanism is label free, applicable to a variety of biomarker types, and able to detect multiple biomarkers simultaneously in various biofluids. A microfluidic flow cell has been fabricated on a polymer substrate to enable point-of-use/care UV measurement of target biomarkers. The overall sensor combines sample dispensing and fluid transport to the detection location with optical absorption measurements with a UV light emitting diode (LED) and photodiode. The biomarker concentration is indicated as a function of photocurrent generated at the target wavelength.

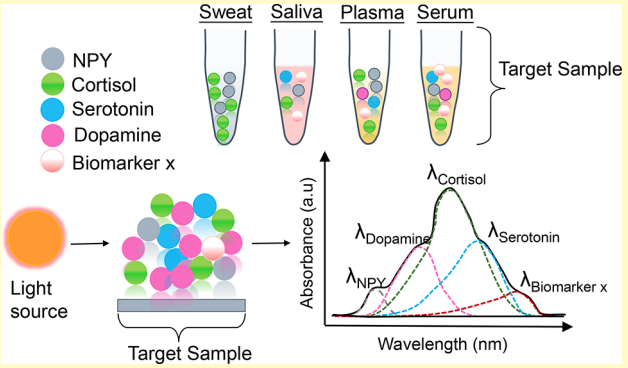

KEYWORDS: *biomarkers, UV spectroscopy, optical sensor, point-of-care, stress detection, biofluids, optoelectronics*

Allostatic stress is very harmful to health, having the potential to permanently alter the human immune system. Physiological and psychological consequences due to exposure to acute or chronic stress[1] can be vast and detrimental, manifesting in various physical and chemical ways.[2] Some of the harmful effects due to exposure of prolonged periods of stress are depression,[3] neurological disorder or breakdown, cardiothoracic disease,[4,5] weight loss or gain,[6] and hyperglycemia.[7] Key biomarkers that have been associated with stress include cortisol,[8] serotonin,[9] norepinephrine[10] (NE), epinephrine,[11] neuropeptide Y[12] (NPY), and brain derived neurotropic factor[13] (BDNF). Regularly monitoring the concentration of these biomarkers in different body fluids (such as plasma, sweat, urine, saliva) provides stress assessment and evaluation of an individual's cognitive ability and their physical condition.[14,15] Laboratory-based biomarker analysis is well developed and provides sensitive measurement of their concentration. However, the associated instrumentation is complex, time-consuming, and expensive, requiring lab space and trained personnel for system operation. Point-of-care/use (PoC/PoU) detection of stress biomarkers seeks to provide simpler, faster, and less expensive instrumentation that can be directly used by a concerned individual, but without the accuracy of laboratory testing. The concentrations of stress biomarkers in bodily fluids and various methods for their PoC/PoU detection have recently been reviewed by Steckl and Ray.[14] The recognition of the stress biomarkers of interest is typically provided by biomolecules, such as antibodies[16−18] and nucleic acid aptamers.[19,20] Many of these techniques utilize a "label" that is attached to the molecule of interest in order to provide a measurable signal. Examples of labeled detection include the use of Au nanoparticles for colorimetric (plasmonic) detection,[21,22] chemiluminescent labels such as enzymes,[23,24] fluorescent labels such as lanthanide atoms or compounds,[25,26] and magnetic nanoparticles.[27,28] Label-free detection is an attractive alternative because it does not require processing of the biofluid sample after it has been obtained. However, few such

Received: February 11, 2019
Accepted: March 22, 2019
Published: March 22, 2019

DOI: 10.1021/acssensors.9b00301
ACS Sens. 2019, 4, 1346−1357

approaches have been implemented to date for PoC/PoU. Sinha et al.[29] describe an innovative simple setup for detection of hydrocortisone in buffer media implemented in a traditional cuvette. Stevens et al.[30] report a surface plasmon biosensor for detection of cortisol in saliva, implemented on an Au surface.

In this Article, we report on the label-free detection of several key stress-related biomarkers in buffer solution and in different body fluids using specific molecular optical absorbance of the biomarkers in the near-ultraviolet (UV) region. UV spectroscopy, which has been utilized for protein quantitation,[31] has several attractive features: it is rapid and convenient, can be performed directly on the sample without adding an external label, and provides a linear relationship between concentration and absorbance; additionally, the sample can be recovered after measurement. Human biofluids are complex, containing multiple strands of proteins, lipids, amino acids, and other components. Human blood is the most complex among all proteomes,[32] containing almost 289 proteins[33] with molecular weight from 5 to 600 kDa, each of different size and function,[34] along with the presence of electrolytes, waste products, dissolved gases, and water. Some biomarkers exist in bound form in whole blood owing to their molecular structure. Cortisol is a prime example, with a high percentage bound to albumin and CBG protein.[35] A percentage of serotonin remains platelet bound,[36] and some portions of NE and epinephrine are bound to plasma proteins. Peripheral noninvasive biofluids (sweat, urine, saliva) are less complex in nature and generally do not bind biomarker molecules. The molecular structure of proteins and organic molecules determine their UV absorbance.[37] Proteins generally display a characteristic near-UV absorption spectrum with absorption peaks in the vicinity of 280 and 200 nm.[38] UV absorption spectra obtained for the stress biomarkers discussed in this Article have primary and secondary absorption peaks in the range of 190−400 nm. UV spectroscopy performed on the target ("stress") sample exhibits characteristic absorption peaks whose wavelengths identify the biomarkers present, with the peak amplitude being related to the biomarker concentration. In the control ("no stress") sample, the characteristic peaks are absent. Biomarker concentrations investigated in this section are close to normal physiological range.

An optical microfluidic sensor has been designed for point of use implementation of UV absorption of the biomarkers. Figure 1a illustrates the basic approach for an optical microfluidic sensor based on UV absorption. The sensor is fabricated on a UV transparent hydrophilic substrate and can be integrated with a miniature UV light emitting diode (LED) light source and photodiode detector for providing an electronic readout of the signal. Figure 1b shows the sensor schematic, including the flow cell into which the fluid is dispensed for measurement. Key device design parameters are channel height (for optimizing the optical path length), sample volume, and polymer UV transparency. The illustrated device is compact and portable, can replace the cuvette in a PoC unit, and has avenues of further miniaturization.

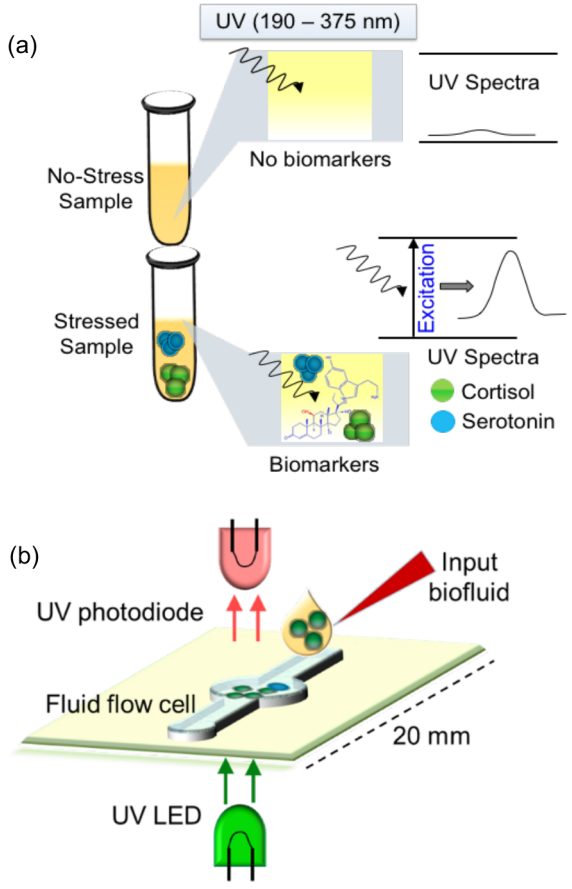

Figure 1. Optical absorption approach for label-free biomarker detection: (a) basic absorption function; (b) integration approach.

EXPERIMENTAL SECTION

Materials and Instruments. Cortisol protein (human; >98%) and brain derived neurotropic factor (BDNF; human; >98%) were purchased from Fitzgerald Industries (MA, USA); serotonin (≥98.0%), neuropeptide Y (NPY; human; ≥95%), norepinephrine (≥98%), epinephrine (≥98%), dopamine hydrochloride, orexin A (human, ≥97%), and α-amylase (human saliva, 300−1500 units/mg) were purchased from Sigma-Aldrich (St. Louis, MO). Biomarker solvents (deionized water, hydrochloric acid, ethanol, acetic acid, calcium chloride, phosphate buffer solution) were purchased from ThermoFisher Scientific (Pittsburgh, PA). 0.9% NaCl solution (ThermoFisher Scientific) was used as primary buffer for all biomarker characterization in buffer solution. Artificial eccrine perspiration (stabilized pH: 4.5) and artificial urine were purchased from Pickering Laboratories (California, USA). Salivette (human saliva extraction) devices were obtained from Sarstedt (Germany). BSA (≥96.0%, lyophilized powder) and albumin (≥96.0%, recombinant, lyophilized powder) were purchased from Sigma-Aldrich (St. Louis, MO). Human plasma and serum (single donor) were obtained from Innovative Research (Novi, MI). Cortisol ELISA kit (plasma and serum) was purchased from Fitzgerald Industries (55R-IB79135). Protein purification (particle sizes: >10, >30, >50, and >100 kDa) of plasma and serum was performed using Amicon Ultra 0.5 mL centrifugal filter devices (Millipore, Billerica, MA, USA). UV fused quartz microvolume cuvettes were purchased from Thor Laboratories (Ann Arbor, MI, USA). UV−vis spectroscopy was performed in a Lambda 900 UV/vis/NIR Spectrophotometer (PerkinElmer, Waltham, MA, USA) and a NanoDrop One Microvolume UV−vis Spectrophotometer (NanoDrop Inc., ThermoFisher Scientific). Protein removal from plasma and serum was performed using an Accuspin Micro17 Micro centrifuge (ThermoFisher Scientific, Pittsburgh, PA). Zeonor film ZF14 (100 μm thickness) was purchased from Zeon Chemicals (Louisville, KY). Acrylic sheets (4 mm thickness) were purchased from US Plastic Corp (Lima, Ohio). LEDs (280NM, 40 M, SMD, part no. VLMU60CL00-280-125CT-ND) and photodiodes (245-400NM TO46, part no. MTPD3650D-1.4) were obtained from Digi key (Thief River Falls, MN). A Universal Laser Systems VLS3.50 laser cutting machine was used for

DOI: 10.1021/acssensors.9b00301
ACS Sens. 2019, 4, 1346−1357

patterning the acrylic and Zeonor films. All materials were used as received without any further modifications.

Sample Preparation for Biomarker Detection in Buffer. Biomarkers were dissolved in their respective solvents and serially diluted to achieve the target concentrations. NPY stock solution (1 mg/mL) was prepared in deionized water and then serially diluted to concentrations of 10, 8, 6, 4, 2, and 1 μg/mL. The remaining stock solution was divided and stored at −20 °C in separate aliquots for subsequent reproducibility tests. Dopamine hydrochloride stock solution (0.1 mg/mL) was initially prepared in deionized water and then serially diluted to concentrations of 5, 4, 3, 2, and 1 μg/mL solutions with 0.9% NaCl solution. Aqueous solutions of dopamine change color to black over time due to dopamine self-polymerization forming polydopamine particles. Hence, fresh samples of dopamine were prepared before each spectroscopic measurement. Cortisol was dissolved in 2% ethanol aqueous solution for a concentration of 0.1 mg/mL as stock solution and then serially diluted in buffer medium (0.9% NaCl solution) to concentrations of 5, 4, 3, 2, 1, and 0.5 μg/mL. Stock solutions of serotonin, norepinephrine, and epinephrine were prepared in 2.5% HCl aqueous solutions for concentrations of 0.1 mg/mL. Serially diluted solutions were then prepared in buffer medium to concentrations ranging from 4 μg/mL down to 0.125 μg/mL. BDNF protein was dissolved in deionized water to a concentration of 1 mg/mL and then diluted to concentrations of 10 and 5 μg/mL. Orexin A was dissolved in 10% acetic acid aqueous solution to a concentration of 0.1 mg/mL and then serially diluted in buffer medium to concentrations of 0.5, 0.4, 0.3, 0.2, and 0.1 μg/mL. α-Amylase stock solution was prepared in a 30 mM $CaCl_2$ PBS solution to a concentration of 2 mg/mL. Serial dilutions were then prepared in buffer medium at concentrations from 1.5 to 0.5 mg/mL. Control samples for UV measurements contained the parent solution minus the target biomarker. For simultaneous detection of serotonin, cortisol, and dopamine, respective volumes from individual stock solutions (0.1 mg/mL) were added to a sample volume of 1 mL one by one for a final concentration of each biomarker of 3, 2, 1, and 0.5 μg/mL. For simultaneous detection of biomarkers from the amine group, samples from all three stock solutions were mixed with buffer solution for final concentrations of serotonin, dopamine, and norepinephrine [A1: 0.2 μg/mL, 2 ng/mL, 0.2 ng/mL; A2: 0.3 μg/mL, 4 ng/mL, 0.3 ng/mL; A3: 0.4 μg/mL, 5 ng/mL, 0.4 ng/mL; A4: 0.5 μg/mL, 6 ng/mL, 0.5 ng/mL; A5: 0.6 μg/mL, 8 ng/mL, 0.6 ng/mL]. The control sample contained an equivalent mixture of solvents as the target sample minus the biomarkers and was used as baseline for each measurement. A sample volume of 100 μL was used for all cases. All UV absorption spectroscopy measurements were performed using the NanoDrop One spectrophotometer with fused quartz cuvettes. Spectrometer baseline calibration and UV absorption measurements with buffer solutions were performed with $n > 4$ iterations. Good reproducibility was observed. Spectra from individual experiments are reported in this manuscript.

Sample Preparation for Biomarker Detection in Body Fluids. Cortisol stock solution was prepared at a concentration of 0.1 mg/mL (in 2% ethanol + 0.9%NaCl solution) and then serially diluted to concentrations of 0.2, 0.3, 0.4, 0.6, and 0.8 μg/mL in artificial sweat. For detection in urine, artificial urine was 50% diluted with 0.9% NaCl solution; cortisol was added from a stock solution for final concentrations of 20, 15, 10, 5, and 1 μg/mL. Saliva samples from human subjects (n = 2 healthy volunteers; samples collected from each volunteer before the afternoon meal on 3 nonconsecutive days) were collected using Salivette collection devices. The device consists of a cotton swab, which was chewed by the subject for 1 min. It was then reinserted into the container and centrifuged at 1000 rpm for 1 min to remove food particles, impurities, and mucus, providing clear saliva samples for the experiments. The collected saliva was spiked with cortisol to concentrations of 5, 4, 3, 2, and 1 μg/mL. As-received commercial serum and plasma (human, single donor) were analyzed for cortisol using ELISA, with concentrations ranging from 12 to 16 μg/dL. For cortisol in plasma and serum, the following sample sets were prepared and analyzed: Set 1: unpurified whole plasma and serum (as received); Sets 2, 3, 4, and 5: protein-purified plasma and serum: removal of particle size >100 kDa (Set 2), particle size >50 kDa (Set 3), particle size >30 kDa (Set 4), and particle size >10 kDa (Set 5). For protein removal, the plasma was treated with Amicon Ultra centrifugation cells. 500 μL of plasma and serum was centrifuged at 14 000 rpm for 10 min. The filtrate was collected for experiments. Purified plasma/serum was spiked with cortisol to achieve concentrations of 5, 10, 20, 40, 60, 80, and 100 μg/mL. Three different batches of single donor human plasma/serum were tested. Serotonin stock solution (0.1 mg/mL concentration in 2.5% HCl/saline solution) was used for artificially spiking 50 kDa purified plasma and serum to achieve concentrations between 10 and 100 μg/mL with a 20 μg/mL interval. Simultaneous detection of serotonin and cortisol was investigated in 50 kDa protein purified plasma. For this purpose, equivalent concentrations of serotonin (from stock solution of 0.1 mg/mL in 2.5%HCl + 0.9%NaCl media) and cortisol (from stock soln. of 0.1 mg/mL in 2.5% HCl + 0.9% NaCl media) were added to plasma samples for final concentrations of 20, 40, 60, 80, and 100 μg/mL for both cortisol and serotonin.

Device Fabrication. Devices were fabricated using plastic (acrylic) and transparent cyclo-olefin polymer (COP, commercially available as Zeonor-ZF14, 100 μM thickness). A schematic of the device cross section is shown in Figure 2a. A stack design was chosen involving three simple processing steps followed by assembly and lamination. COP has good transparency in the UV region. It is thin, flexible, hydrophilic, easy to handle, and biocompatible and has relatively low cost. Five separate microfluidic channels (2 mm channel width, active detection region width 5 mm) were laser milled into a 20

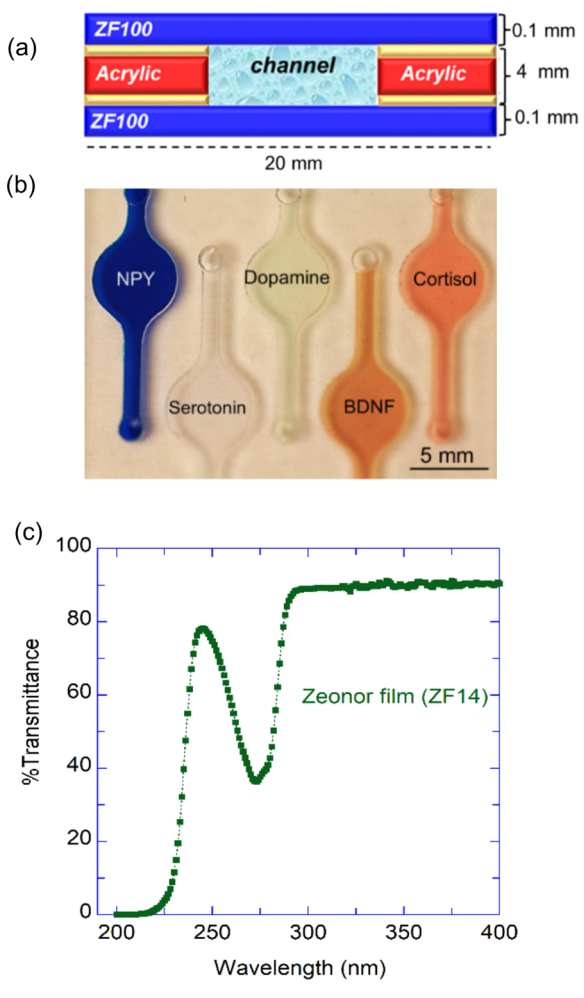

Figure 2. Optical flow cell: (a) cross-section; (b) photograph of assembled unit; (c) optical transmission spectrum for 100 μm Zeonor film.

DOI: 10.1021/acssensors.9b00301
ACS Sens. 2019, 4, 1346−1357

mm × 20 mm acrylic sheet (VLS3.50, Universal Laser Systems Inc., Scottsdale, AZ). Since the channel height determines the optical path length and the sample volume, which directly impacts absorption intensity, acrylic sheets of several thicknesses were tested to achieve maximum limit of detection. The 4 mm channel height was found to be optimum in terms of optical absorbance, input sample volume, and laser milling compatibility. Laser power and speed were optimized for a smooth vector cut along the channel edges. The dimensions of the measurement (central) region of the flow cell were selected to accommodate the LED and photodiode (PD) dimensions. The top and bottom polymer layers were cut into 20 mm × 20 mm pieces to fit the acrylic substrate. Fluid inlet and air vent openings were laser milled into the polymer layer. Low laser power was used to prevent damage to the polymer film. All the layers were cleaned with DI water and mechanical scrubbing using clean wipes to remove any foreign particle, which might inhibit adhesion between the layers. Pressure sensitive adhesive was applied on both sides of the acrylic chip, followed by assembly of all three layers and lamination. A photograph of the assembled device is shown in Figure 2b. The optical transmission spectrum of a 100 μm Zeonor (ZF14) film is shown in Figure 2c. The dispensed input sample volume is 100 μL, and sample volume in the active detection region is ~ 65 μL. The flow cells were typically stored in open air in a clean room environment at ambient temperature for periods from 1 to 15 days prior to testing. No loss of performance was observed with storage time.

RESULTS AND DISCUSSION

UV Characterization (Buffer). Many organic compounds have absorption bands in the near-UV spectrum associated with conjugated C═C and C═N double bonds that produce strong $\pi-\pi^*$ interactions (at wavelengths of ~185−190 nm) and weaker n−π * interactions from C═O and N═O bonds (at 280−300 nm).[39] The absorption bands for specific compounds can shift to longer wavelengths due to substitutions in the aromatic system or to longer and more complex polymers.[40] Figure 3 shows UV absorption spectra of biogenic amines (the catecholamines dopamine, norepinephrine, epinephrine, and serotonin) at several concentrations in HCl solutions. The catecholamines have a very similar molecular structure: each has one benzene ring and a terminally attached amine group. Norepinephrine contains one OH group, while epinephrine contains an OH and a terminal CH_3 group. The catecholamines are formed as a part of a process chain starting from hydroxylation of the essential amino acid tyrosine.[41] Dopamine is the first product of the metabolic process chain, followed by formation of norepinephrine and epinephrine. These three biomarkers have very similar absorption characteristics: a dominant peak at λ_1 = 204 nm and secondary peaks at λ_2 = 217 and λ_3 = 278 nm, with absorbance levels in the order of $\lambda_1 > \lambda_2 > \lambda_3$.

Because of the overlap between the λ_1 and λ_2 peaks, the profiles have been deconvolved in order to more accurately identify the individual peak wavelengths and respective absorbance values (Figure S1). Some differences between the catecholamines were observed in the relative strengths of the three absorption peaks. The ratio between the combined absorbance of the secondary peaks (λ_2 + λ_3) and the absorbance of the primary peak (λ_1) is approximately 0.64 for dopamine, while it is ~0.5 for norepinephrine and epinephrine. This difference in peak ratio could be utilized for identification of specific biomarkers. Serotonin is formed through hydroxylation and decarboxylation of the essential amino acid tryptophan and contains two fused rings.[42] The UV absorption profile of serotonin, shown in Figure 3d, contains the three peaks of the catecholamines (203.5, 220, 275 nm) plus a fourth peak (λ_4) at 299 nm. In the case of serotonin, the absorbances at λ_1 and λ_2 are approximately equal, unlike the

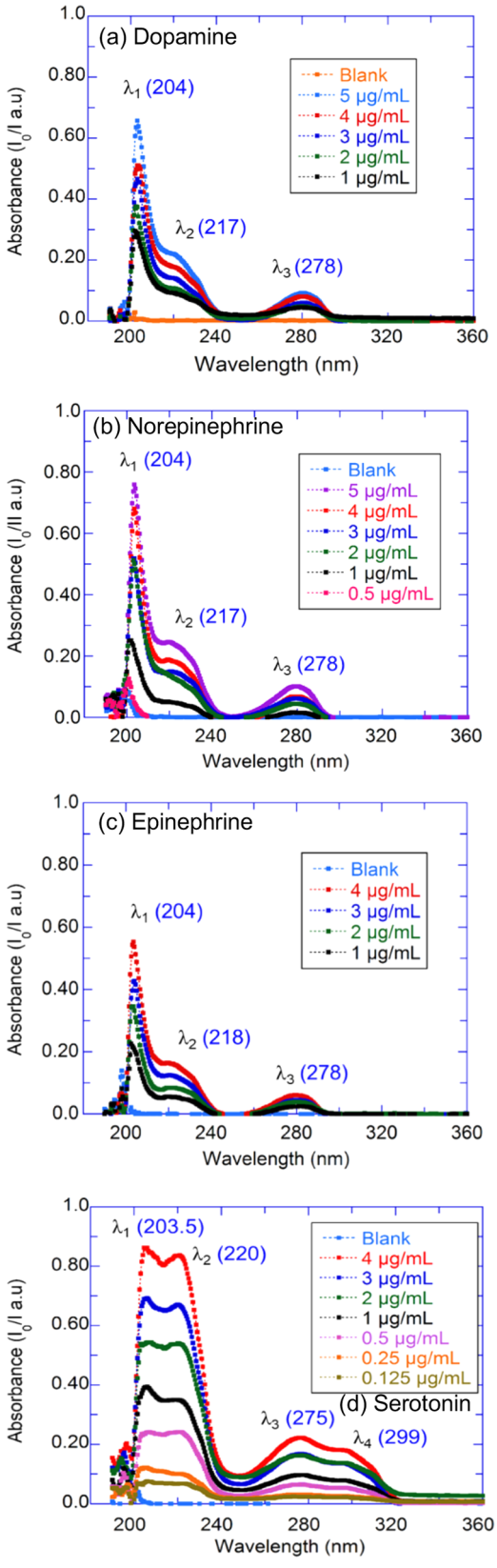

Figure 3. UV absorption spectra of amines as a function of concentration in HCl solutions: (a) dopamine; (b) norepinephrine; (c) epinephrine; (d) serotonin. For deconvolved spectra, see Figure S1.

DOI: 10.1021/acssensors.9b00301
ACS Sens. 2019, 4, 1346−1357

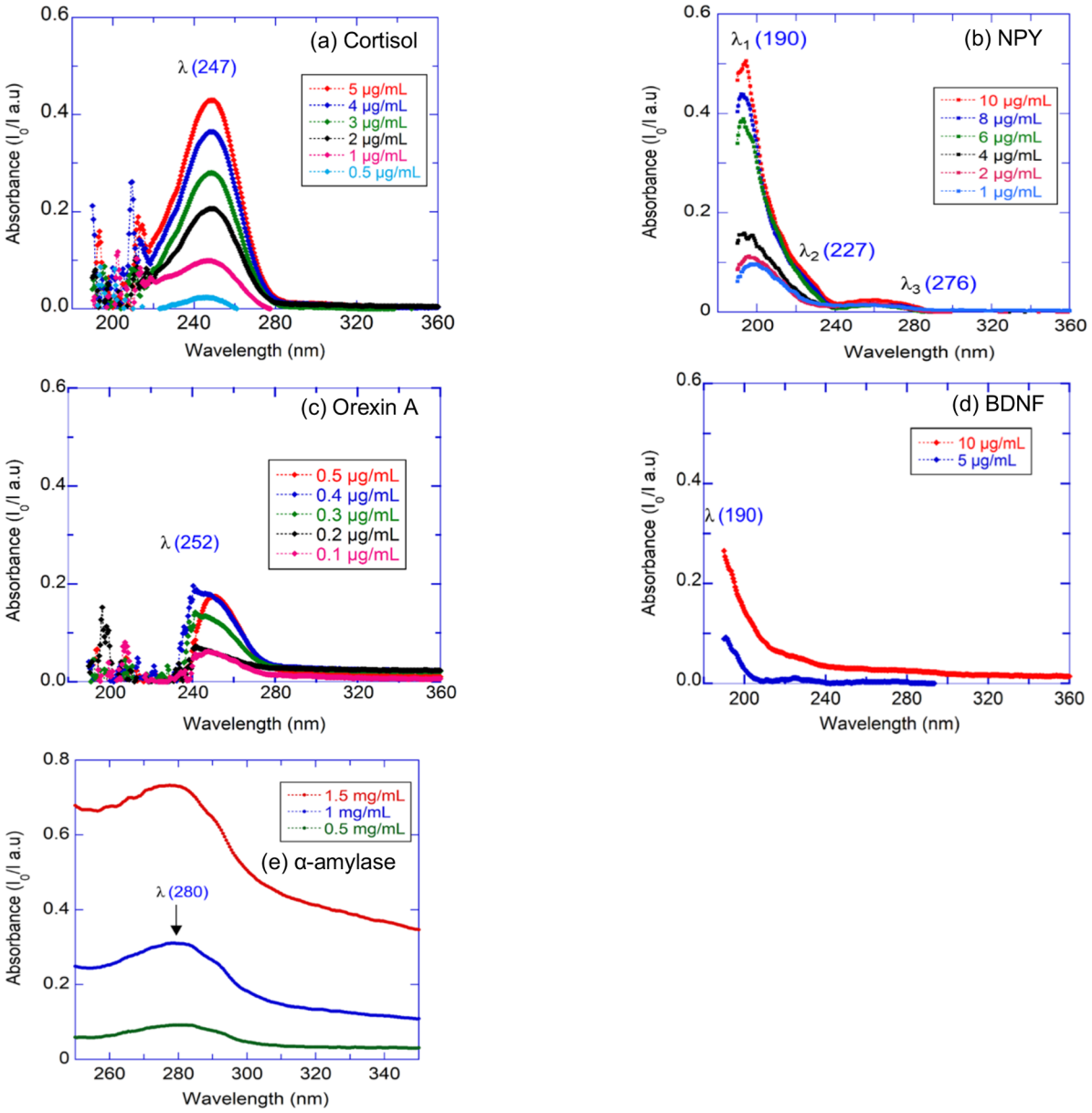

Figure 4. UV absorption spectra of steroids, peptides, and an enzyme in conventional solvents: (a) cortisol (ethanol); (b) NPY (aq.); (c) orexin A (acetic acid); (d) BDNF (aq.); (e) salivary α-amylase.

case of the simpler amines. The concentration dependence of the absorption peaks for dopamine, norepinephrine, and epinephrine indicate a limit of detection (LoD) of ~0.5−1 μg/mL level. For serotonin, the current LoD is ~0.1 μg/mL, which is compatible with the normal physiological range in blood of 0.2−0.4 μg/mL. UV−vis absorption of cortisol and the larger molecular biomarkers NPY (fragment 3-36), BDNF, and orexin A is shown in Figure 4. Cortisol displays a single major peak at ~247 nm detectable down to ~0.5 μg/mL, which is close to the healthy physiological range (0.1−0.3 μg/mL). NPY (in aqueous solution) has a dominant peak at ~190 nm and minor absorption peaks at 227 and 276 nm. The main NPY peak at 190 nm displays a clear monotonic dependence on NPY concentration over the measured range (1−10 μg/mL), as shown in the spectra of Figure 4b. Absorption spectra of orexin A (Figure 4c) indicate a clear UV peak at ~252 nm at a concentration of 0.5 μg/mL. The absorption decreases monotonically with concentration down to ~0.2 μg/mL, accompanied by increasing noise level and a possible blue shift in peak wavelength. Preliminary optical absorbance measurements of BDNF (in aqueous solution) samples do show a concentration dependence in the low μg/mL ranges. However, the peak absorption wavelength was not determined as it appears to be below the 190 nm lower limit of the spectrometer. For completion, the UV absorption spectrum of the enzyme biomarker salivary α-amylase, which has a strong peak at 282 nm, has also been included (Figure 4e). The absorption peaks of various stress biomarkers are tabulated in Figure 5. The dominant peak for each biomarker is shown in bold. While some overlap between the dominant peaks of several biomarkers does exist in the ~190−210 nm region, the combination of primary and secondary peaks appears to allow for the identification of most biomarkers.

The biomarkers (oxytocin, cortisol, orexin A) with main peaks in the 230−255 nm range are significantly separated from the amine-related peaks at ~200 nm, allowing their ready

DOI: 10.1021/acssensors.9b00301
ACS Sens. 2019, 4, 1346−1357

Biomarker	MW (Da)	Ave Molar Abs Coeff - ε (M^{-1} cm^{-1})	ε std dev. (M^{-1} cm^{-1})	Wavelength (nm)
Dopamine	153	22821	3072	~204
Norepi.	169	28549	1800	~204
Serotonin	176	33,329	3,744	~204
Epineph.	183	28570	3074	~204
Cortisol	362	24,412	1,961	247

Biomarker	Absorption Peak Wavelengths (nm)		
α-Amylase	**282**		
BDNF	**190**		
Cortisol	**247**		
Dopamine*	**204**	217	278
Epinephrine*	**204**	217	278
Norepinephrine*	**204**	218	278
Serotonin	**204**	**220**	275/299
NPY	**190**	227	276
Orexin A	**252**		
Oxytocin	190	**232**	

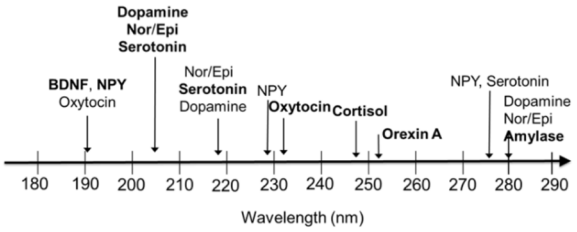

Figure 5. Optical absorption peak wavelengths and molar absorption coefficients of selected biomarkers; dominant peaks are shown in bold; ∗: peak wavelengths from deconvolved spectra (see Figure S1).

identification. The molar absorption coefficients of several biomarkers were calculated on the basis of their absorbance at specific peak wavelengths: 204 nm for dopamine, norepinephrine, epinephrine, and serotonin; 247 nm for cortisol. The absorption coefficient generally increases with increasing complexity and molecular weight of the biomarker molecules. Figure 6 shows integrated values of signal intensity (of all absorption peaks present in each spectrum) vs concentration for each of the biomarkers investigated. A roughly linear trend in absorption levels with increasing concentration is observed over ∼ 2 orders of magnitude.

A preliminary investigation of using UV absorbance to determine the simultaneous presence of multiple biomarkers was performed. UV absorbance spectra of samples containing a combination of cortisol and two amines (serotonin and dopamine) are shown in Figure 7a at concentrations from 0.5 to 3 μg/mL. As expected, since dopamine and serotonin both absorb at ∼200 and ∼220 nm, their combined absorbance values are observed at these wavelengths in these spectra.[38] The longer wavelength absorption peaks of cortisol, dopamine, and serotonin are observed at ∼247, 282, and 301 nm, respectively. For improved visualization of the individual characteristic peaks, spectral deconvolution was performed with Origin Pro peak analysis software.[43] A deconvolution

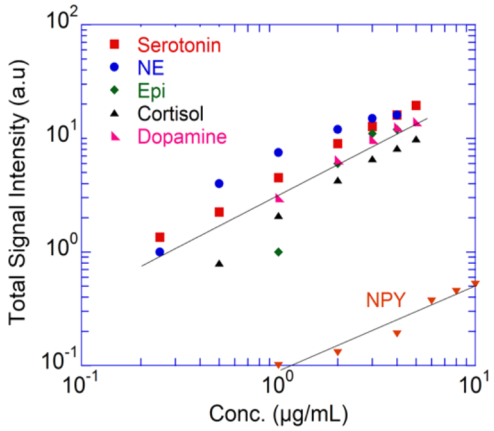

Figure 6. Integrated signal intensity vs biomarker concentration.

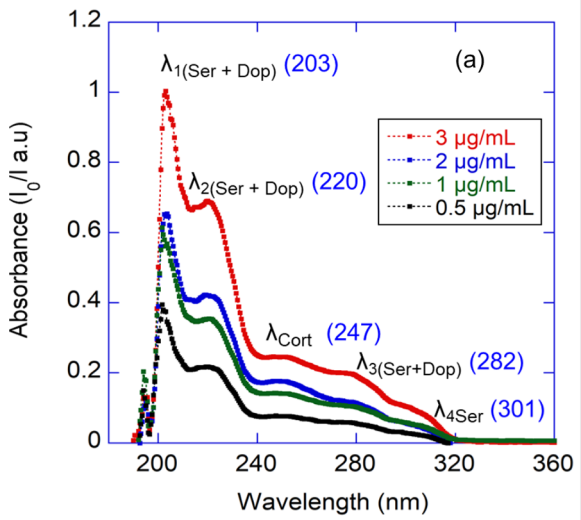

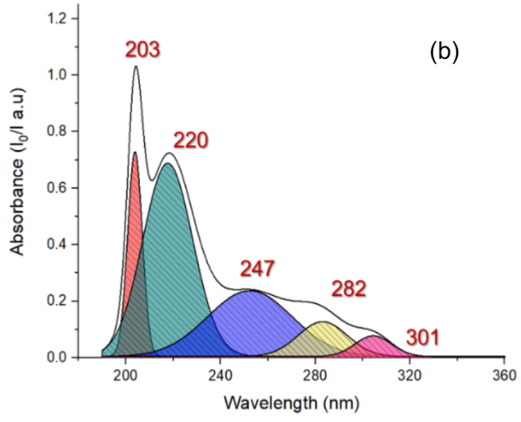

Figure 7. Simultaneous detection of cortisol and amine biomarkers (serotonin, dopamine); (a) UV spectra; (b) deconvolved spectra (conc., 3 μg/mL).

example is shown in Figure 7b for combined spectra obtained at a sample concentration of 3 μg/mL. Clear identification is obtained for the individual absorbance peaks at the target wavelengths, confirming the feasibility of simultaneous detection of cortisol and amine biomarkers when present in the same sample. Signal deconvolution implemented on raw spectrum data recognizes absorbance peaks at wavelengths within ±3 nm, which is considered to be a generally acceptable

DOI: 10.1021/acssensors.9b00301
ACS Sens. 2019, 4, 1346−1357

range. Furthermore, changes in solvent pH or temperature might also cause minor changes in peak wavelength., This effect is particularly observed in the case of serotonin. For a serotonin-only solution (in saline buffer and 2.5% HCl media), λ_3 and λ_4 absorbance peaks occur at 275 and 299 nm, as shown in Figure 3d. However, for the mixed biomarker samples, the λ_3 peak wavelength ranges from 278 to 282 nm, while the λ_4 peak wavelength is observed between 300 and 305 nm. It is also possible that the sample medium for the combined biomarkers (containing saline buffer, 2% ethanol, DI water, 2.5% HCl) affects the absorption wavelengths. Cortisol is a primary stress hormone that is present at relatively higher concentrations in most body fluids during all times and under various kinds of stress. The separation between the primary cortisol absorption peak and the amine peaks is advantageous and enables a simpler optical detection process. The amine biomarkers have similar absorption spectra owing to the similarity of their molecular structure, and when they are simultaneously present in a sample, their absorption peaks overlap. It is also possible that the sample medium for the combined biomarkers (containing saline buffer, 2% ethanol, DI water, 2.5% HCl) affects the absorption wavelengths. Cortisol is a primary stress hormone that is present at relatively higher concentrations in most body fluids during all times and under various kinds of stress. The separation between the primary cortisol absorption peak and the amine peaks is advantageous and enables a simpler optical detection process. The amine biomarkers have similar absorption spectra owing to the similarity of their molecular structure, and when they are simultaneously present in a sample, their absorption peaks overlap. Figure 8a shows UV spectra of samples containing a combination of serotonin, dopamine, and norepinephrine in concentrations within the healthy physiological range for each biomarker (see concentrations in the Sample Preparation for Biomarker Detection in Buffer section). In these combined samples, absorbance peaks of all three biomarkers are observed at 203, 220, and 278 nm, while absorbance at 301 nm serves as an identification of the presence of serotonin. The serotonin-only spectra (Figure 3d) show an absorbance ratio of $\lambda_{203}/\lambda_{220} \sim 1$, while the combined amine sample spectra in Figure 8 exhibit a corresponding ratio of ~1.5. This confirms that the combined absorbance also contains contributions from dopamine and norepinephrine in the sample.

Since during an event of stress there is increased release of all amine-based biomarkers, their combined increased signal intensity at 203, 220, and 278 nm can be used for the overall screening of the occurrence of stress. However, for a combined amine sample (both physiological or stressed), serotonin concentration can be isolated and quantified by analyzing the absorption at $\sim\lambda_{299}$. In a serotonin-only spectrum, the absorbance ratios are $\lambda_{203}/\lambda_{299} \sim 4.2$, $\lambda_{220}/\lambda_{299} \sim 4$, and $\lambda_{275}/\lambda_{299} \sim 1.25$. Buffer, being a pure medium, absorption peak wavelengths, and ratios between observed peak wavelengths should be used as the "standard". By knowing the absorbance intensity at λ_{299}, one can make an estimation of λ_{203}, λ_{220}, and λ_{275}, which will give a serotonin concentration in amine-only samples.

UV Characterization (Biofluid). The ability of the UV absorption detection method to selectively detect target biomarkers was also investigated in the more complex natural biofluid environment, where molecules, such as proteins and lipids, can interfere with the results for the target biomarker. For experiments in biofluids, several experiments were selected

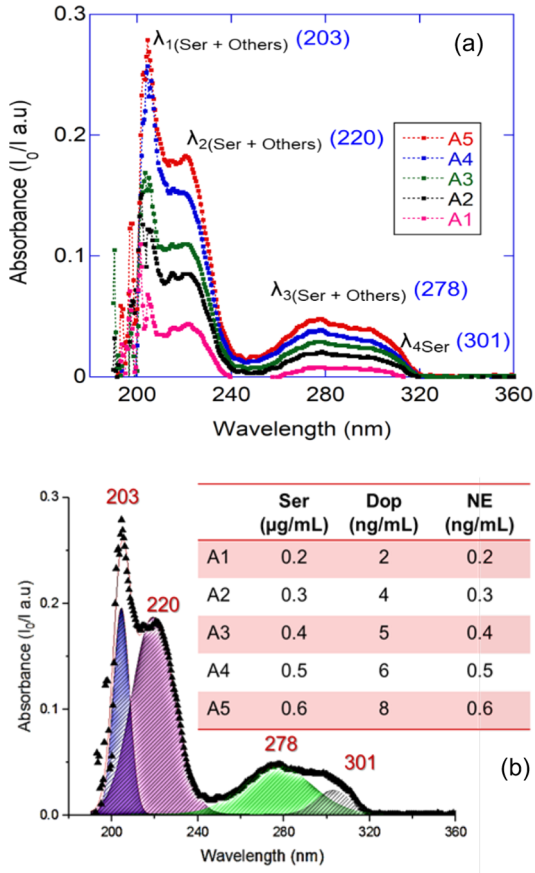

	Ser (μg/mL)	Dop (ng/mL)	NE (ng/mL)
A1	0.2	2	0.2
A2	0.3	4	0.3
A3	0.4	5	0.4
A4	0.5	6	0.5
A5	0.6	8	0.6

Figure 8. Simultaneous detection of multiple amines (serotonin, dopamine, and norepinephrine): (a) UV spectra; (b) deconvolved spectra (concentration A5).

with focus on: (a) cortisol detection (in sweat, saliva, urine, plasma, and serum) due to its presence in all biofluids at a high concentration range; (b) serotonin detection (in plasma and serum) since it is the highest concentration stress biomarker found in whole blood. Single donor human plasma and serum were used. Saliva experiments were pursued with samples from human volunteers. For sweat experiments, a commercial product ("artificial" sweat) was purchased, which contains all 19 essential amino acids, 7 abundant minerals, and 4 abundant metabolites with pH of 4.5 and has close resemblance with human sweat.[44] Similarly, for urine, an artificial version was used, with composition that matches human urine[44] in terms of chemical composition and pH. Cortisol detection was first pursued in plasma and serum. Cortisol interaction with plasma protein was analyzed by comparing the absorption spectra from unpurified, undiluted whole plasma and serum (Set 1: as received, no purification) with those that were purified with 100, 50, 30, and 10 kDa filters (Sets 2, 3, 4, 5). Figure 9 shows integrated absorption profiles of cortisol in plasma (Figure 9a) and serum (Figure 9b). For whole serum and whole plasma, no significant cortisol absorption peak is observed for concentrations lower than 80 μg/mL. After removing proteins with size >100 kDa, improved signal resolution leads to a detection sensitivity of 20 μg/mL. Further removal of protein size >50 kDa results in a detection limit of 10 μg/mL. Protein purification for particle size >30 kDa and >10 kDa leads to detection of cortisol at concentrations as low as ~5 μg/mL. As observed, optical absorption increases with increasing protein

DOI: 10.1021/acssensors.9b00301
ACS Sens. 2019, 4, 1346−1357

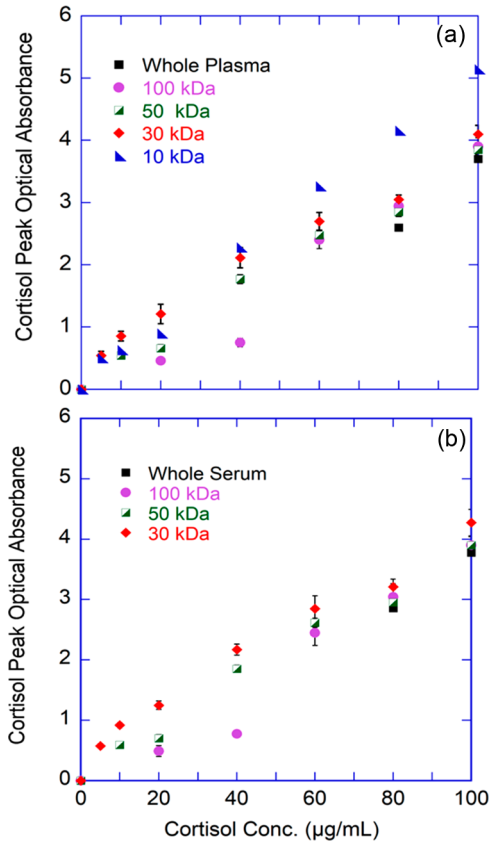

Figure 9. Effect of protein removal on cortisol detection in human plasma (a) and serum (b).

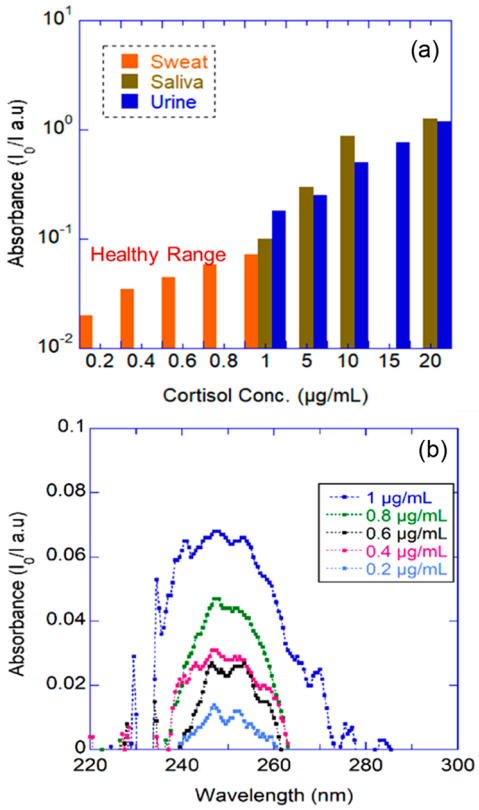

Figure 10. Cortisol detection in noninvasive biofluids (sweat, saliva, urine): (a) integrated cortisol absorbance signal intensity vs concentration; (b) individual cortisol UV spectra (in sweat) at several concentrations.

removal. In human plasma and serum, 80−90% cortisol is bound to corticosteroid-binding globulin (110 kDa); 5−10% binds to albumin (66.5 kDa), and approximately 3−10% is free cortisol.[35,45] This explains the increased cortisol signal observed with protein removal at increasingly lower molecular weight. The absorption spectrum of undiluted human plasma below 300 nm shows high absorbance at ∼210 and 280 nm (Figure S2) due to inherent high concentration of proteins. For eliminating the strong background absorption of plasma samples, a control sample (plasma without spiked cortisol) was used for spectrometer baseline calibration. This way, a relatively small change due to cortisol absorbance was observable. The detection of cortisol in noninvasive body fluids (sweat, saliva, urine) was also investigated. Figure 10a shows a summary of integrated total absorbance vs cortisol concentration in sweat, saliva, and urine. Sweat contains traces of albumin, adipsin, creatinine, lipids, and amino acids with a considerable concentration of electrolytes and minor concentration of proteins.[46] While the concentration of cortisol in sweat is lower than that in plasma, it is compensated by the lower protein concentration (which tends to bind the lipophilic cortisol molecule). As a result, cortisol concentrations as low as 0.2 μg/mL are detectable in sweat, as shown in the spectrum in Figure 10b. The composition of urine is more complex compared to sweat and saliva.[51] Human urine has been reported to contain 158 compounds of varying concentration, such as high concentration of urea, electrolytes, organic and inorganic compounds, hormones, amino acids, and nitrogenous compounds, such as creatine and creatinine. Among 158 chemicals in urine, 68 compounds have individual concentration greater than 0.01 g/L.[52] Key inorganic salts found in urine at fairly high concentrations are NaCl, KCl, K_2SO_4, $MgSO_4$, $KHCO_3$, and K_3PO_4 (concentration ranging from 0.2 to 8 g/L). The concentration of nitrogenous compounds, such as urea is ∼13 g/L, while creatinine is 1.5 g/L. Several free and bound amino acids are present in urine, such as taurine, threonine, serine, asparagine, glycine, alanine, cystine, valine, leucine, tyrosine, phenylalanine, histidine, etc.[53] Ammonium salts such as lactate, hippurate, citrate, urate, and glucuronate are present at ∼1 g/L concentration. Proteins such as traces of globulin protein are also released in urine,[54] though the concentration is fairly small and largely dependent upon physiological health of the individual.[55] Hence, the ability of cortisol to be detected in urine without strong signal interference (due to presence of proteins) is higher than in plasma or serum. Commercially purchased artificial urine closely mimics human urine composition in terms of pH and organic and inorganic constituents. Undiluted and 50% diluted urine were tested. Due to the presence of urea, creatine, and creatinine at fairly high concentrations, undiluted urine produced a rather noisy spectrum between 200 and 240 nm. On the other hand, the 50% diluted urine sample delivered a usable spectrum (with reduced noise) and was therefore selected for cortisol measurements (absorption spectra shown in Figure S3a−c). The presence of cortisol has been detected in human saliva using UV spectroscopy. The normal concentration of cortisol in saliva is about 100× lower than in sweat; hence, it would not be possible to implement this technique in real time at the physiological range, unless other sample processing steps (such as preconcentration) are applied. However, for proof of concept, cortisol in the

DOI: 10.1021/acssensors.9b00301
ACS Sens. 2019, 4, 1346−1357

concentration range of 1−20 μg/mL was tested in human saliva (Figures 10a and S3d). In general, samples of saliva, urine, and sweat can be processed through microfiltration membranes for removal of macroparticles. Samples obtained at the point of low stress can be used as control sample for spectrometer baseline calibration. One key hurdle in implementing this technique for cortisol detection in biofluids, particularly plasma/serum, is the presence of steroid hormone isoforms of cortisol, such as prednisolone, progesterone, estradiol, and testosterone. Table 1 includes some of their

Table 1. Properties of Corticosteroid Hormonal Isoforms[a]

Hormone	Structure, Formula Mol Wt. (g/mol)		Conc. in plasma (μg/dL)	λ_{max} (nm)	Ref.
Cortisol	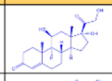	$C_{21}H_{30}O_5$ 362.46	~14	247	(Steckl and Ray 2018)
Prednisolone	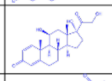	$C_{21}H_{28}O_5$ 360.45	~11	242	(Ashok, Prakash et al. 2011)
Progesterone	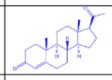	$C_{21}H_{30}O_2$ 314.46	~ 0.2	240	Pubchem - Progesterone
Estradiol	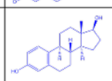	$C_{18}H_{24}O_2$ 272.38	~ 0.005	225, 280	Pubchem - Estradiol
Testosterone	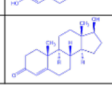	$C_{19}H_{28}O_2$ 288.42	~ 0.5	238	Pubchem - Testosterone

[a]Cortisol,[14] prednisolone,[47] progesterone,[48] estradiol,[49] and testosterone[50].

key characteristics: molecular weight, concentration, and UV absorption wavelength. Among these cortisol isoforms, the presence of prednisolone in both plasma and urine would particularly cross interfere with cortisol. λ_{max} of prednisolone and cortisol are in close vicinity, and the presence of both in a sample would result in spectral broadening or widening. In this case, calculating the signal derivative would help in isolating close peaks. The concentrations of other steroid hormones such as testosterone and progesterone predominantly found in plasma are substantially lower than cortisol and are also gender specific. Hence, they would not create a deviating result. Any biosensor designed to detect cortisol in biofluids has the potential to respond to the presence of these hormones, because of their structural similarity. Another important stress biomarker is serotonin. Serotonin in blood exists in both free and bound form[56] to platelets[57] and to a few other coagulation factors,[58] such as vWf protein. To observe the feasibility of using UV spectroscopy for detection of serotonin in plasma/serum, experiments were performed using whole plasma/serum and 50 kDa purified plasma/serum [Set 1: whole plasma, 50 kDa purified plasma] and serum [Set 2: whole serum, 50 kDa purified serum]. From previous experiments involving cortisol detection, it was observed that the LoD using 50 kDa protein purified plasma/serum was similar to those obtained with 30 and 10 kDa protein purification. Hence, for proof of concept of serotonin detection, the 50 kDa purification step was chosen. Peak absorbance at λ = 278 nm for plasma and serum [both whole and 50 kDa purified] is presented in Figure 11a as a function of serotonin concentration. Since 50 kDa purified plasma is mostly devoid of platelets and serum is additionally devoid of most other coagulation proteins, minimum binding activity between

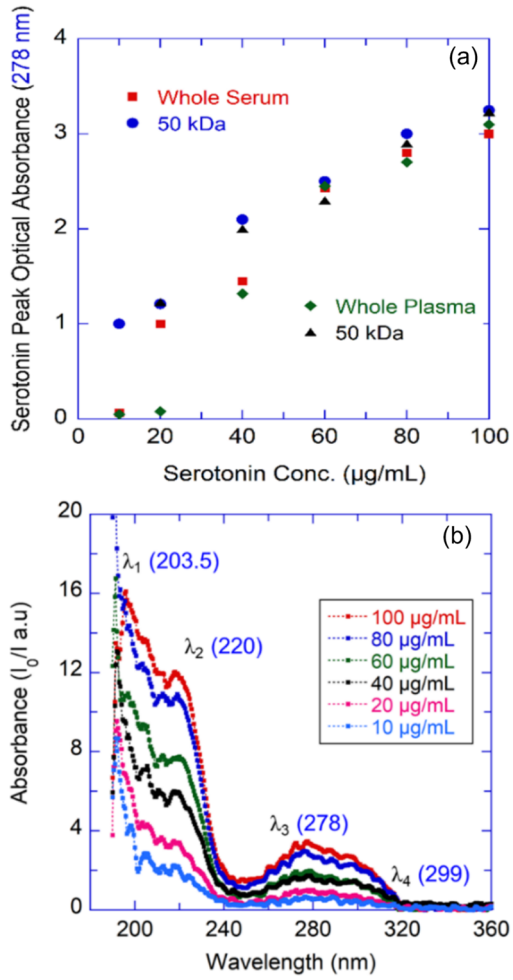

Figure 11. Serotonin detection in human plasma and serum: (a) peak absorbance at 280 nm vs serotonin concentration in whole and 50 kDa purified plasma and serum; (b) absorption spectra for several concentrations in 50 kDa purified plasma.

serotonin and proteins is expected. Indeed, for serotonin concentrations higher than ~50 μg/mL, no difference in absorption signal between the purified and unpurified plasma and serum in plasma is observed. At lower serotonin concentrations, the purified medium resulted in higher signal than its unpurified counterpart. Individual serotonin absorption spectra in 50 kDa purified plasma are shown in Figure 11b at several concentrations. The serotonin absorption peaks at wavelengths (λ) of 203, 220, 278, and 299 nm are clearly visible. While the noise level in the spectra is much reduced after 50 kDa protein purification, it is expected that further improved results can be obtained by removal of lower molecular weight proteins from the plasma. Preliminary experiments were conducted for simultaneous detection of serotonin and cortisol in plasma using UV spectroscopy. Since individual detection of cortisol and serotonin using 50 kDa purified plasma showed reproducible and promising results with similar LoDs, purified plasma was chosen for the proof of concept experiments. The resulting absorption spectra show (Figure S4a) well separated and identifiable peaks for serotonin (203.5, 220, 278, and 299 nm) and cortisol (247 nm) at concentrations above ~40−50 μg/mL. The noise level present in the spectra can be reduced by protein filtering at a smaller molecular weight. The deconvolved absorption spectra

DOI: 10.1021/acssensors.9b00301
ACS Sens. 2019, 4, 1346−1357

allows better visualization of the individual absorption peaks, as shown in the example contained in Figure S4b.

Device Characterization. Several experiments were carried out to determine and optimize the performance of the microfluidic optical detection unit. As shown above in the device schematic in Figure 1b, the central detection region of the optical flow cell was sandwiched between a UV-emitting (280 nm) LED and a photodiode detector. The LED was powered by a DC power source at 5.5 V bias, and the photodiode was biased using a LabView controlled DC power source at 4 V. LED, PD I–V characteristics, emission spectra, and responsivity spectra can be found in Figures S5 and S6. The test was initiated by measuring the photocurrent associated with a control sample, followed by samples of different analyte concentration. The flow cell channel was flushed with DI water 2 times before each measurement. The photocurrent was recorded at 0.1 s intervals for 45 s. Photodiode current measurements were obtained for different concentrations of serotonin and dopamine (from zero to 100 μg/mL) in the optical flow cell. Figure 12a shows the photocurrent as a function of serotonin concentration in saline buffer. As observed, the photocurrent monotonically decreases with serotonin concentration, due to increasing absorbance in the flow cell with increasing concentration. The maximum photocurrent difference between the control (no serotonin) sample and the 100 μg/mL serotonin sample is ~ 40 nA. The photocurrent difference between the control sample and the 1 μg/mL serotonin sample is ~0.015 μA or 15 nA/(μg/mL). Photocurrent changes at this level can be detected by several types of microelectronic sensing circuits. The LOD for serotonin using this detection technique is likely to be well below 1 μg/mL, which would approach the physiological range in plasma and urine. A similar trend is observed for photocurrent vs dopamine concentration in saline buffer (Figure 12b). The photocurrent difference between control (no dopamine) sample and the 1 μg/mL dopamine sample is ~18 nA, which holds promise that the LOD can go below 1 μg/mL (near the physiological range in urine). Fairly good reproducibility was obtained for multiple iterations (n > 4) for both serotonin and dopamine. Further improvement in flow cell substrate material and optoelectronics can yield significant improvement in LoD. The current version of optical flow cell reported in this manuscript has ~45% transmission at 280 nm (Figure 2c). Materials with higher UV transparency such as quartz (~80% transmission at 280 nm) would reduce the LoD to ~0.6–0.7 μg/mL for both serotonin and dopamine with the current set of LED and PD (responsivity 0.05 A/W). Quartz slides can be procured in various thicknesses (50 μm to 1 mm), which can help in building thinner and more compact flow cells. Current versions of flow cell fabrication cost in a lab-based environment are approximately 50 cents/flow cell. Using quartz would tentatively increase it to ~$5/flow cell (in small quantities), which would still be in a reasonable range. For optoelectronics, the photodiode (GaP) used for this study has a responsivity of ~50 mA/W at 280 nm. There are photodiodes available with higher responsivity (part no.: SD012-UVB-011-ND; GaN photodiode; responsivity of 100 mA/W at 280 nm; part no.: SD012-UVC-011; AlGaN photodiode; responsivity of 60 mA/W at 280 nm). Using these photodiodes in association with a quartz flow cell can lead to an LoD of <0.3 μg/mL for both serotonin and dopamine. A related cost calculation and information on the material source for future experiments are provided in the Supporting Information.

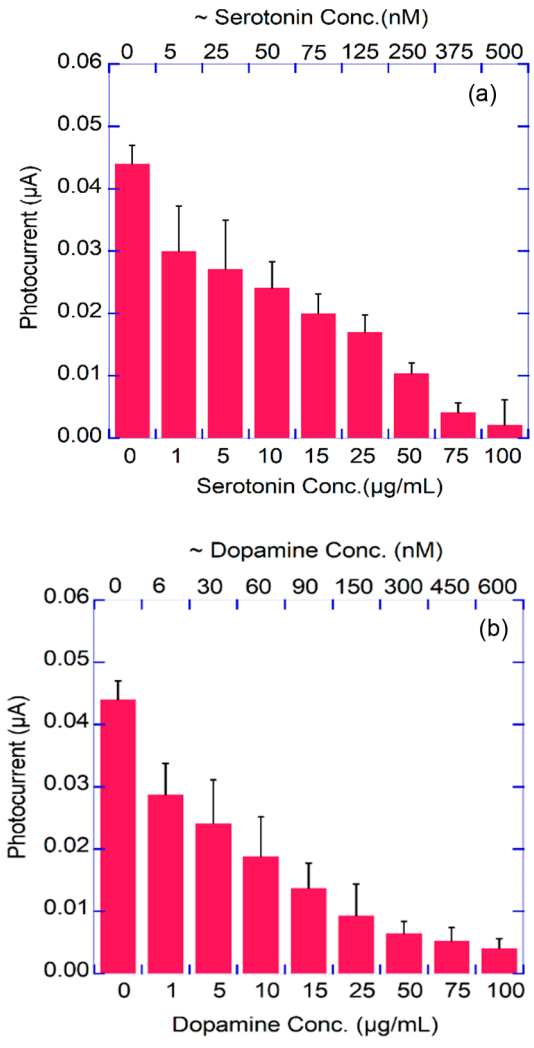

Figure 12. Photocurrent level vs biomarker (in saline buffer) concentration: (a) serotonin; (b) dopamine. n = 4 for both biomarkers.

SUMMARY AND CONCLUSION

The optical properties of key biomarker molecules (hormones and neurotransmitters) associated with stress have been reported. These biomarkers display characteristic absorption peaks in the near-UV range (~190–400 nm) that allow for their detection in biological fluids (e.g., plasma, sweat, saliva, urine., etc.). Cortisol (362 Da) has a unique absorption peak at 247 nm.

The UV absorption profile of serotonin (175 Da) contains a series of four absorption peaks (203, 220, 275, and 299 nm). The amine group of biomarkers (catechols) [dopamine (153 Da), norepinephrine (169 Da), and epinephrine (183 Da)] displays similar absorption peaks at 203, 218, and 278 nm, owing to their structural similarity. NPY (4.3 kDa) generates characteristic absorption peaks at 190, 229, and 276 nm, while BDNF (14 kDa) has a peak at 190 nm. The absorption level of the peaks associated with these biomarkers follows a similarly increasing trend with concentration. Measurements of single and combined biomarkers in buffer solution and different biofluids were performed. For example, the cortisol limit of

DOI: 10.1021/acssensors.9b00301
ACS Sens. 2019, 4, 1346–1357

detection (LOD) in sweat using UV absorption is ~0.2 μg/mL (0.5 μM), which falls in the healthy physiological range (0.1–0.4 μg/mL). An optical microfluidic sensor for PoC/PoU biomarker detection based on UV absorption has been designed and fabricated. The sensor consists of a microfluidic flow cell fabricated on a UV transparent substrate combined with optoelectronic components for performing the optical characterization: UV LED as light source and UV photodiode as detector. Preliminary sensor results for serotonin and dopamine indicate an LOD of <1 μg/mL. It is anticipated that, with a few improvements in the optoelectronics components and their integration, the result will be significant LOD improvement.

■ ASSOCIATED CONTENT

Supporting Information

The Supporting Information is available free of charge on the ACS Publications website at DOI: 10.1021/acssensors.9b00301.

Spectral characterization (including signal deconvolution) in plasma, urine, and saliva for cortisol and serotonin; UV LED/PD characteristics (PDF)

■ AUTHOR INFORMATION

Corresponding Author

*E-mail: a.steckl@uc.edu.

ORCID

Prajokta Ray: 0000-0001-6262-9021

Andrew J. Steckl: 0000-0002-1868-4442

Notes

The authors declare no competing financial interest.

■ ACKNOWLEDGMENTS

This work was supported by the National Science Foundation and by the industrial members of the Center for Advanced Design and Manufacturing of Integrated Microfluidics (NSF I/UCRC IIP-1738617) and by UES Inc. (S-104-000-001) as a subcontract from AFRL (FA8650-15-C-6631). The authors gladly acknowledge the assistance of ALine Inc. for providing the flow cell components. The authors also acknowledge many helpful discussions with Stefano Begolo, Leanna Levine, Jorge Chavez, and Craig Murdock.

■ REFERENCES

(1) Steptoe, A.; Hamer, M.; Chida, Y. The effects of acute psychological stress on circulating inflammatory factors in humans: a review and meta-analysis. *Brain, Behav., Immun.* **2007**, *21* (7), 901–912.

(2) Sapolsky, R. M. Why stress is bad for your brain. *Science* **1996**, *273* (5276), 749–750.

(3) Chaouloff, F.; Berton, O.; Mormède, P. Serotonin and stress. *Neuropsychopharmacology* **1999**, *21*, 28S–32S.

(4) Taelman, J.; Vandeput, S.; Spaepen, A.; Van Huffel, S. Influence of mental stress on heart rate and heart rate variability. In *4th European conference of the international federation for medical and biological engineering*; Springer: 2009; pp 1366–1369.

(5) Bruno, A.; Biller, J.; Adams, H.; Clarke, W.; Woolson, R.; Williams, L.; Hansen, M. Acute blood glucose level and outcome from ischemic stroke. *Neurology* **1999**, *52* (2), 280–280.

(6) Kivimäki, M.; Head, J.; Ferrie, J.; Shipley, M.; Brunner, E.; Vahtera, J.; Marmot, M. Work stress, weight gain and weight loss: evidence for bidirectional effects of job strain on body mass index in the Whitehall II study. *Int. J. Obes.* **2006**, *30* (6), 982–987.

(7) McCowen, K. C.; Malhotra, A.; Bistrian, B. R. Stress-induced hyperglycemia. *Crit. Care Clin.* **2001**, *17* (1), 107–124.

(8) Burke, H. M.; Davis, M. C.; Otte, C.; Mohr, D. C. Depression and cortisol responses to psychological stress: a meta-analysis. *Psychoneuroendocrinology* **2005**, *30* (9), 846–856.

(9) Chaouloff, F. Serotonin, stress and corticoids. *J. Psychopharmacol.* **2000**, *14* (2), 139–151.

(10) Simeon, D.; Knutelska, M.; Smith, L.; Baker, B. R.; Hollander, E. A preliminary study of cortisol and norepinephrine reactivity to psychosocial stress in borderline personality disorder with high and low dissociation. *Psychiatry Res.* **2007**, *149* (1–3), 177–184.

(11) Wright, P. H.; Malaisse, W. J. Effects of epinephrine, stress, and exercise on insulin secretion by the rat. *Am. J. Physiol.* **1968**, *214* (5), 1031–1034.

(12) Heilig, M. The NPY system in stress, anxiety and depression. *Neuropeptides* **2004**, *38* (4), 213–224.

(13) Martinowich, K.; Manji, H.; Lu, B. New insights into BDNF function in depression and anxiety. *Nat. Neurosci.* **2007**, *10* (9), 1089–1093.

(14) Steckl, A. J.; Ray, P. Stress Biomarkers in Biological Fluids and Their Point-of-Use Detection. *ACS Sensors* **2018**, *3* (10), 2025–2044.

(15) Piazza, J. R.; Almeida, D. M.; Dmitrieva, N. O.; Klein, L. C. Frontiers in the use of biomarkers of health in research on stress and aging. *Journals of Gerontology Series B: Psychological Sciences and Social Sciences* **2010**, *65B* (5), 513–525.

(16) Mitchell, J. S.; Lowe, T. E.; Ingram, J. R. Rapid ultrasensitive measurement of salivary cortisol using nano-linker chemistry coupled with surface plasmon resonance detection. *Analyst* **2009**, *134* (2), 380–386.

(17) Ishchenko, A.; Wacker, D.; Kapoor, M.; Zhang, A.; Han, G. W.; Basu, S.; Patel, N.; Messerschmidt, M.; Weierstall, U.; Liu, W.; et al. Structural insights into the extracellular recognition of the human serotonin 2B receptor by an antibody. *Proc. Natl. Acad. Sci. U. S. A.* **2017**, *114* (31), 8223–8228.

(18) An, J. H.; Choi, D.-K.; Lee, K.-J.; Choi, J.-W. Surface-enhanced Raman spectroscopy detection of dopamine by DNA Targeting amplification assay in Parkisons's model. *Biosens. Bioelectron.* **2015**, *67*, 739–746.

(19) Hauke, A.; Kumar, L. S.; Kim, M.; Pegan, J.; Khine, M.; Li, H.; Plaxco, K.; Heikenfeld, J. Superwetting and aptamer functionalized shrink-induced high surface area electrochemical sensors. *Biosens. Bioelectron.* **2017**, *94*, 438–442.

(20) Dalirirad, S.; Steckl, A. J. Aptamer-based lateral flow assay for point of care cortisol detection in sweat. *Sens. Actuators, B* **2019**, *283*, 79–86.

(21) Anker, J. N.; Hall, W. P.; Lyandres, O.; Shah, N. C.; Zhao, J.; Van Duyne, R. P. Biosensing with plasmonic nanosensors. In *Nanoscience and Technology: A Collection of Reviews from Nature Journals*; World Scientific: 2010; pp 308–319.

(22) Zeng, S.; Yong, K.-T.; Roy, I.; Dinh, X.-Q.; Yu, X.; Luan, F. A review on functionalized gold nanoparticles for biosensing applications. *Plasmonics* **2011**, *6* (3), 491.

(23) Roda, A.; Mirasoli, M.; Michelini, E.; Di Fusco, M.; Zangheri, M.; Cevenini, L.; Roda, B.; Simoni, P. Progress in chemical luminescence-based biosensors: a critical review. *Biosens. Bioelectron.* **2016**, *76*, 164–179.

(24) Marquette, C. A.; Blum, L. J. Chemiluminescent enzyme immunoassays: a review of bioanalytical applications. *Bioanalysis* **2009**, *1* (7), 1259–1269.

(25) Li, Z.; Wang, Y.; Wang, J.; Tang, Z.; Pounds, J. G.; Lin, Y. Rapid and sensitive detection of protein biomarker using a portable fluorescence biosensor based on quantum dots and a lateral flow test strip. *Anal. Chem.* **2010**, *82* (16), 7008–7014.

(26) Venkatraman, V.; Steckl, A. J. Integrated OLED as excitation light source in fluorescent lateral flow immunoassays. *Biosens. Bioelectron.* **2015**, *74*, 150–155.

(27) Georganopoulou, D. G.; Chang, L.; Nam, J.-M.; Thaxton, C. S.; Mufson, E. J.; Klein, W. L.; Mirkin, C. A. Nanoparticle-based detection in cerebral spinal fluid of a soluble pathogenic biomarker for

DOI: 10.1021/acssensors.9b00301
ACS Sens. 2019, 4, 1346–1357

Alzheimer's disease. *Proc. Natl. Acad. Sci. U. S. A.* **2005**, *102* (7), 2273−2276.
(28) Lu, A. H.; Salabas, E. e. L.; Schüth, F. Magnetic nanoparticles: synthesis, protection, functionalization, and application. *Angew. Chem., Int. Ed.* **2007**, *46* (8), 1222−1244.
(29) Sinha, R.; Vabbina, P. K.; Ahmadivand, A.; Karabiyik, M.; Gerislioglu, B.; Pala, N. Ultraviolet LED based compact and fast cortisol detector with ultra high sensitivity. In *2016 IEEE SENSORS*; IEEE: 2016; pp 1−3.
(30) Stevens, R. C.; Soelberg, S. D.; Near, S.; Furlong, C. E. Detection of cortisol in saliva with a flow-filtered, portable surface plasmon resonance biosensor system. *Anal. Chem.* **2008**, *80* (17), 6747−6751.
(31) Noble, J. E.; Bailey, M. J. Quantitation of protein. In *Methods in Enzymology*; Elsevier: 2009; Vol. *463*, pp 73−95.
(32) Ray, S.; Reddy, P. J.; Jain, R.; Gollapalli, K.; Moiyadi, A.; Srivastava, S. Proteomic technologies for the identification of disease biomarkers in serum: advances and challenges ahead. *Proteomics* **2011**, *11* (11), 2139−2161.
(33) Anderson, N. L.; Anderson, N. G. The human plasma proteome history, character, and diagnostic prospects. *Mol. Cell. Proteomics* **2002**, *1* (11), 845−867.
(34) Putnam, F. *The Plasma Proteins V3: Structure, Function, and Genetic Control*; Elsevier: 2012.
(35) Heyns, W.; Van Baelen, H.; De Moor, P. Study of steroid-protein binding by means of competitive adsorption: application to cortisol binding in plasma. *Clin. Chim. Acta* **1967**, *18* (3), 361−370.
(36) Somerville, B. W. Platelet-bound and free serotonin levels in jugular and forearm venous blood during migraine. *Neurology* **1976**, *26* (1), 41−41.
(37) Pelton, J. T.; McLean, L. R. Spectroscopic methods for analysis of protein secondary structure. *Anal. Biochem.* **2000**, *277* (2), 167−176.
(38) Noble, J. E. Quantification of protein concentration using UV absorbance and Coomassie dyes. In *Methods in Enzymology*; Elsevier: 2014; Vol. *536*, pp 17−26.
(39) Perkampus, H.-H. *UV-VIS Spectroscopy and its Applications*; Springer Science & Business Media: 2013.
(40) Mabry, T. J.; Markham, K. R.; Thomas, M. B. The ultraviolet spectra of isoflavones, flavanones and dihydroflavonols. In *The systematic identification of flavonoids*; Springer: 1970; pp 165−226.
(41) Daubner, S. C.; Le, T.; Wang, S. Tyrosine hydroxylase and regulation of dopamine synthesis. *Arch. Biochem. Biophys.* **2011**, *508* (1), 1−12.
(42) Keszthelyi, D.; Troost, F.; Masclee, A. Understanding the role of tryptophan and serotonin metabolism in gastrointestinal function. *Neurogastroenterol. Motil.* **2009**, *21* (12), 1239−1249.
(43) *Origin Pro Peak Analyzer*. https://www.originlab.com/index.aspx?go=products/origin/dataanalysis/peakanalysis (accessed 09/02/2018).
(44) Pickering Laboratories. https://www.pickeringtestsolutions.com/artificial-urine/.
(45) Le Roux, C.; Chapman, G.; Kong, W.; Dhillo, W.; Jones, J.; Alaghband-Zadeh, J. Free cortisol index is better than serum total cortisol in determining hypothalamic-pituitary-adrenal status in patients undergoing surgery. *J. Clin. Endocrinol. Metab.* **2003**, *88* (5), 2045−2048.
(46) Sonner, Z.; Wilder, E.; Heikenfeld, J.; Kasting, G.; Beyette, F.; Swaile, D.; Sherman, F.; Joyce, J.; Hagen, J.; Kelley-Loughnane, N.; et al. The microfluidics of the eccrine sweat gland, including biomarker partitioning, transport, and biosensing implications. *Biomicrofluidics* **2015**, *9* (3), No. 031301.
(47) Ashok, R.; Prakash, P.; Tamil Selvan, R. Development and validation of analytical method for estimation of prednisolone in bulk and tablets using UV-Visible spectroscopy. *Int. J. Pharm. Pharm. Sci.* **2011**, *3* (4), 184−186.
(48) Pubchem. *Progesterone*; https://pubchem.ncbi.nlm.nih.gov/compound/progesterone.
(49) Pubchem. *Estradiol*; https://pubchem.ncbi.nlm.nih.gov/compound/estradiol.
(50) Pubchem. *Testosterone*; https://pubchem.ncbi.nlm.nih.gov/compound/testosterone.
(51) Taylor, E. N.; Curhan, G. C. Body size and 24-h urine composition. *Am. J. Kidney Dis.* **2006**, *48* (6), 905−915.
(52) Putnam, D. F. *Composition and concentrative properties of human urine*; NASA: Washington, DC, 1971.
(53) Stein, W. H.; Carey, G. C. A chromatographic investigation of the amino acid constituents of normal urine. *J. Biol. Chem.* **1953**, *201*, 45−58.
(54) Sylvester, K. G.; Ling, X. B.; Liu, G. Y.-G.; Kastenberg, Z. J.; Ji, J.; Hu, Z.; Wu, S.; Peng, S.; Abdullah, F.; Brandt, M. L.; et al. Urine protein biomarkers for the diagnosis and prognosis of necrotizing enterocolitis in infants. *J. Pediatr.* **2014**, *164* (3), 607−612.e7.
(55) Wang, T.; Zhou, R.; Gao, L.; Wang, Y.; Song, C.; Gong, Y.; Jia, J.; Xiong, W.; Dai, L.; Zhang, L.; Hu, H. Elevation of Urinary Adipsin in Preeclampsia. *Hypertension* **2014**, *64* (4), 846−851.
(56) Frattini, P.; Cucchi, M. L.; Santagostino, G.; Corona, G. L. A sensitive fluorimetric method for determination of platelet-bound and plasma free serotonin. *Clin. Chim. Acta* **1979**, *92* (3), 353−360.
(57) Cremer, S. E.; Kristensen, A. T.; Reimann, M. J.; Eriksen, N. B.; Petersen, S. F.; Marschner, C. B.; Tarnow, I.; Oyama, M. A.; Olsen, L. H. Plasma and serum serotonin concentrations and surface-bound platelet serotonin expression in Cavalier King Charles Spaniels with myxomatous mitral valve disease. *Am. J. Vet. Res.* **2015**, *76* (6), 520−531.
(58) Dale, G. L.; Friese, P.; Batar, P.; Hamilton, S. F.; Reed, G. L.; Jackson, K. W.; Clemetson, K. J.; Alberio, L. Stimulated platelets use serotonin to enhance their retention of procoagulant proteins on the cell surface. *Nature* **2002**, *415*, 175−178.

DOI: 10.1021/acssensors.9b00301
ACS Sens. 2019, 4, 1346−1357